Preprints (www.preprints.org) | NOT PEER-REVIEWED | Posted: 26 November 2020 doi:10.20944/preprints202011.0670.v1

Article

Material Origins of Accelerated Operational Wear of RD-33 Engine Blades

Adam Kozakiewicz [1], Stanisław Jóźwiak [2], Przemysław Jóźwiak [3] and Stanisław Kachel [1,*]

[1] Military University of Technology, Faculty of Mechatronics, Armament and Aerospace, Institute of Aviation Technology, ul. Kaliskiego 2, 00-908 Warszawa, Poland; adam.kozakiewicz@wat.edu.pl
[2] Military University of Technology, Faculty of Advanced Technology and Chemistry, Institute of Materials Science and Engineering, ul. Kaliskiego 2, 00-908 Warszawa, Poland; stanislaw.jozwiak@wat.edu.pl
[3] Air Force Institute of Technology, ul. Księcia Bolesława 6, 01-494 Warszawa, Poland; przemyslaw.jozwiak@itwl.pl
* Correspondence: stanislaw.kachel@wat.edu.pl; Tel.: +48 261 839 170

Abstract: The structural and strength analysis of the material used to construct such an important engine element as the turbine is of great significance, both at the design stage as well as during tests and expertises related to emergency situations. Bearing in mind the conditions above mentioned, the paper presents the results of research on the chemical composition, morphology and phased structure of the metallic construction material used to produce the blades of the high and low pressure turbine of the RD-33 jet engine, which is the propulsion unit of the MiG-29 aircraft. The data obtained as a result of the material tests of the blades allowed, on the basis of the analysis of chemical composition and phased structure, to determine the grade of the alloy used to construct the tested elements of the jet engine turbine. The structural stability of the material was found to be lower in comparison with engine operating conditions, which manifested itself as a clear decrease in the resistance properties of the blade material. The results obtained can be used as a basis for analyzing the life span of an object or a selection of material replacements, which enable to produce the analyzed engine element.

Keywords: turbine jet engine; material tests; ember-resistant alloys

1. Introduction

The introduction should briefly place the study in a broad context and highlight why it is important. It should define the purpose of the work and its significance. The current state of the research field should be reviewed carefully and key publications cited. Please highlight controversial and diverging hypotheses when necessary. Finally, briefly mention the main aim of the work and highlight the principal conclusions. As far as possible, please keep the introduction comprehensible to scientists outside your particular field of research. References should be numbered in order of appearance and indicated by a numeral or numerals in square brackets, e.g., [1] or [2,3], or [4–6]. See the end of the document for further details on references.

2. Analysis of the state of the issue

Aviation turbine engines must meet very high requirements regarding the criteria of reliability, strength, minimum weight, serviceability, the acceptable period of use in service, noise, ecology and cost-effectiveness [5]. In turbine jet engines, one of the essential components affecting these criteria is the turbine assembly. A turbine assembly is a system that is heavily loaded mechanically and thermally, which is caused by tension and bending of the blades as a result of centrifugal forces, bending and twisting resulting from the exhaust gas mass flow, and which is also caused by high temperature. This results in a number of complex stress states, especially in blade palisades of rotor

Preprints (www.preprints.org) | NOT PEER-REVIEWED | Posted: 26 November 2020 doi:10.20944/preprints202011.0670.v1

wreaths, including the occurrence of variable stress. Therefore, in order to increase the operational properties, the changes in the blade design are made in two ways: by means of changes in design improving the cooling efficiency and by means of changes in the material of the blade matrix as well as in protective coatings protecting from overheating (Figure 1.).

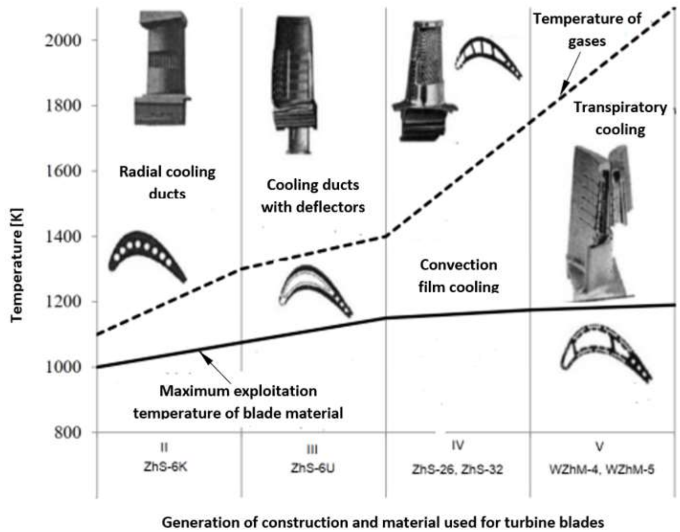

Figure 1. Development of the cooling technology and change in materials used to construct Russian turbine jet engines [1].

The basic parameter characterizing the ember-resistance of nickel-based super alloys intended for the construction of turbine blades of jet engines is their creep resistance. The increase of this parameter depending on the phased structure of the alloy, and in particular the share of γ/γ' phases, reinforcement carbides, Laves phases, etc., is obtained by modifying the chemical composition and morphology of the crystal structure of the blade matrix material. The same also happens in case of Russian superalloys. An increase in creep resistance of materials used to produce turbine blade was obtained by using additives Re and Ta, which, together with directional crystallization (ZhS-26) or monocrystalline crystallization (ZhS-32) allowed, in comparison with alloy ZhS-6U, to significantly increase this parameter (Table 1).

Table 1. Creep resistance of super alloys ZhS [2.].

alloy	σ^{900}_{100} [MPa]	σ^{1000}_{100} [MPa]	σ^{1100}_{100} [MPa]
ZhS-6U	350	170	65
ZhS-26	400	200	85
ZhS-32	480	250	120

Increase of the creep resistance of ZhS-32 alloy according to the authors [2.] allowed to increase the temperature of gases on the blades of the first stage of the turbine from 1263°C (for ZhS-6U-VI alloy [3.]) up to 1400°C. However, due to the acceptable period of use in service of RD-33 engine, prolonged temperature of the blade material exceeding 1100°C is not recommended.

The preservation of these exploitation regimes allowed to extend the acceptable period of use in service of the RD-33 engine blades made of superalloy ZhS-32 from 300 hours (ZhS-6) up to 1000 hours of exploitation. Nevertheless, one must keep in mind that prolonged exposure to hot exhaust gases can lead, especially if the protective coating is damaged, to structural changes within the blade material, thus leading to its destruction. Detailed analysis of the RD-33 engine damage showed that over 42% of the failures were caused by damage to the blades, of which the damages to blades of the first stage of the turbine accounted for over 60% [3.]. The main causes of damages are: gaseous

Preprints (www.preprints.org) | NOT PEER-REVIEWED | Posted: 26 November 2020 doi:10.20944/preprints202011.0670.v1

corrosion at the leading edge, cracks at the leading and trailing edges and also thermo-mechanical damages (Figure 2).

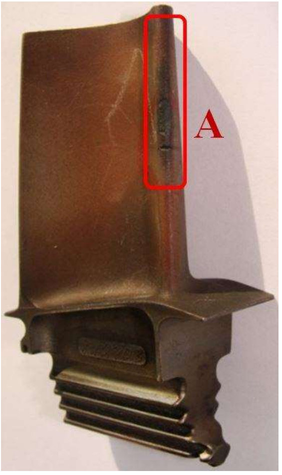

Figure 2. Blade from the rotor wreath of a high-pressure turbine with a marked zone (A) of gas corrosion damage and crack damage of the leading edge of the blade.

The scope of application of alloys used to construct blades of the RD-33 engine, and in particular the creep resistance depending on temperature and duration of its long-term impact on the material, is best represented by the Larson-Miller parametric coordinates defined by the formula(1) (Figure 8.):

$$P = (T + 273) * (20 + \log t) * 10^{-3} \quad (1)$$

where:

T – temperature [°C]

t – exploitation time [h]

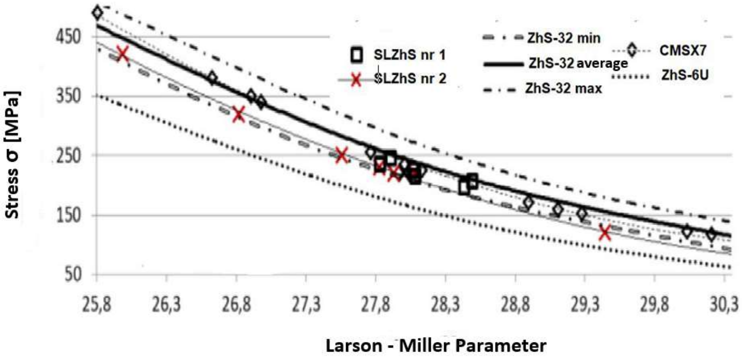

Figure 3. Influence of temperature and exploitation time on the exploitation stress of ZhS alloys used in the construction of engine RD-33 turbine blades, defined by the Larson-Miller parameter P [1.].

Higher permissible exploitation stress of the ZhS-32 alloy compared to ZhS-6U should be explained by a higher volume content of the phase γ' in the material structure, 67% and 57% respectively, as well as its higher thermal stability, caused by Re and Ta additives, which increase the temperature of the solidus from 1240°C (ZhS-6U) up to 1310°C (ZhS-32) [4.]. It is obvious that the long-drawn process of exploitation, linked with the high-temperature influence of exhaust gases, causes the grain coarsening and decrease of the phase γ' content in the blade material structure (Figure 4.).

Preprints (www.preprints.org) | NOT PEER-REVIEWED | Posted: 26 November 2020 doi:10.20944/preprints202011.0670.v1

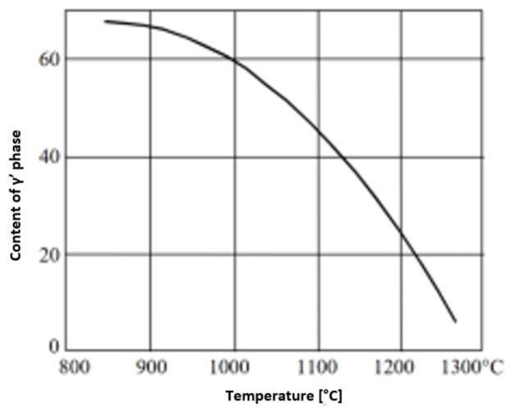

Figure 4. Influence of exploitation temperature on the share of the phase γ' in structure of the ZhS-32 alloy [8.].

These phenomena result in a decrease in strength parameters in nickel-based super-alloys, manifested by a significant decrease in the fatigue strength of the blade material (Figure 5.).

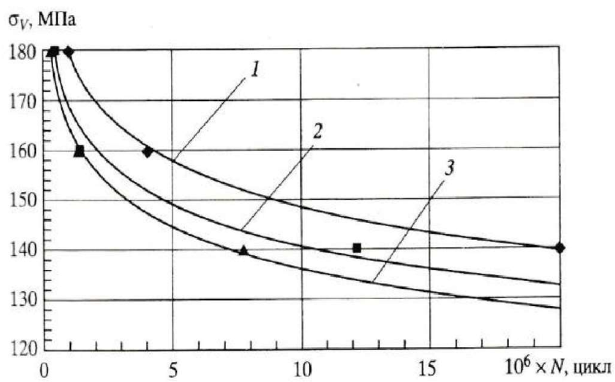

Figure 5. The fatigue curves of turbine blades made of EI-437B, where working time t=0h (1) t=200h (2) and t=400h (3)[6.].

In connection with the above mentioned conditionalities / exploitation and strength rationale, for the purpose of research on the construction of the aircraft engine assemblies in the area of structural analysis, a thorough analysis of material degradation shall be carried out. It must take into account the tests of the grain structure and the chemical composition that determines the phased structure, which directly affects the operational properties, including the mechanical properties that determine the performance of such a complex structure as the modern turbine system. Incorrect use of a given[?] construction material, or incorrect exploitation or other factors causing the limits (resulting from strength calculations) of the applied materials to be exceeded, may lead to a reduction in strength. This, in turn, may lead to damage to the turbine assembly as well as the engine.

The above assumptions are the basis for the research undertaken to determine the causes of premature damages to the blades of the turbine of the RD-33 engine of the MiG-29 airplane, resulting in the necessity to dismount the engines and perform engine overhauls.

2. Sample preparation and test methodology

The mass loads, and in particular the heat loads of the turbine blades caused by the exhaust gas stream coming from the combustion chamber (1560 K) require cooling of this engine component. In the RD-33 motor under analysis, blades of both LPT and HPT are cooled by means of internal channels (Figure 6.), and blades of HPT, due to the higher gas temperature, have also channels for cooling the trailing edge.

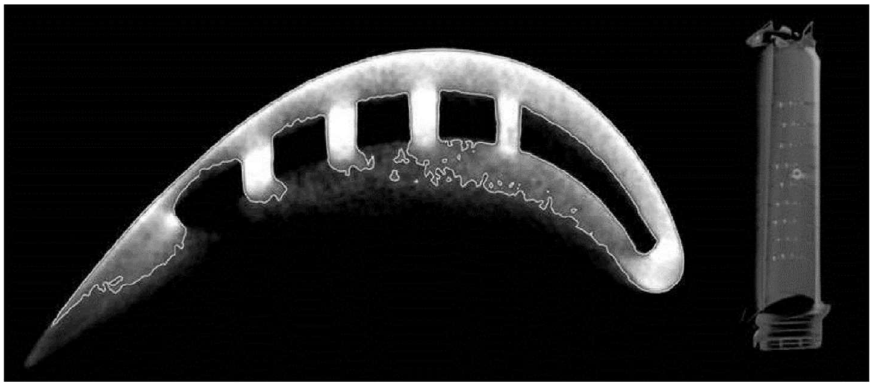

(a)

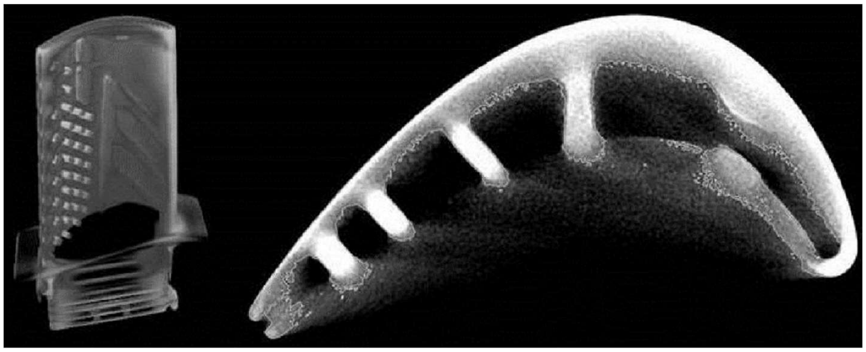

(b)

Figure 6. The shape of the LPT blade (a) and the HPT blade (b) with visible cooling channels, obtained by the computer-based micro-tomography CT.

This blade design poses serious problems in selecting a place to take the strength test specimens to properly perform the static tensile test. Therefore, taking into account the nature of the mechanical loads carried by the material of the component tested, it was assumed that the specimens for the static tensile tests will be cut along the blade feather of the LPT, i.e. in the direction of centrifugal forces, and in case of HPT from the lock material, i.e. the component subjected to the highest mass loads (Figure 7.).

Figure 7. View of specimens cut out, by using the electro-discharge method, of a material of the LPT blade and view of specimens for static tensile testing, cut out oof material of HPT blade and LPT blade.

 doi:10.20944/preprints202011.0670.v1

Nevertheless, the three-dimensional shape with variable cross-sections and curvatures made it impossible to clamp and thus to make the strength specimens with classical machines for cavity machining (edging method machining). Therefore, in order to preserve the assumed shape, dimensions and geometric quality of the surface of the specimens, as well as to minimize the impact of the preparation process on the structural changes of the blade material, the electro-discharge machining was used as the cutting method. All the samples were made by using the electro-discharge wire rod numerically controlled machine and assumed geometric dimensions have been respected.

In order to make microscopic observations to reveal the grain structure of the blade material, metallographic samples were prepared (Figure 8.) by mounting them in a conductive resin and then grinding them with abrasive papers of varying granulation in the range 100⊚1000, and by final polishing with a diamond slurry of polishing powder, using the Struers polishing machine.

Figure 8. Metallographic specimen of material of the LPT blade.

Microscopic observations at magnifications of 100⊚10000 times were made by using the Quanta 3D FEG (SEM/FIB) high resolution scanning microscope, which, in addition to grain structure morphology analysis, also enables, with the use of EDS/WDS/EBSD attachments, complex studies of chemical composition in microareas, as well as analysis of crystallographic orientation.

Since the microanalysis of chemical composition indirectly allows only for identification of the phased structure of the material under investigation, it was necessary to perform X-ray phase analysis (XRD). Identifying the type of crystal lattice and measuring the parameters of the elementary crystal cell allows, in a precise and unambiguous way, for identification of the phased structure of the material under investigation, on which functional properties, including strength properties depend. The phase X-ray analysis was carried out with ULTIMA IV Rigaku diffractometer by using a parallel beam. The measurements were carried out using a cobalt lamp with radiation length CoKα1=1.78892 Å with power 1600W, scanning step 0.02º and scanning speed 2º/min in the angular range 2Θ=20º-140º. The identification of the obtained reflections and the phased analysis were carried out on the basis of the crystallographic database PDF-4.

The evaluation of mechanical properties of the material of the tested blades was based on hardness, microhardness and the static tensile test. Due to the ultrafine grain structure of the tested material, in order to unequivocally confirm the correctness of the hardness measurements, the testing of this strength parameter was carried out using three measurement methods (HBW2.5/187.5, HV10 - Wolpert Wilson Testor and HRC - Rockwell PW 106 hardness meter), and then (using appropriate nomograms enabling comparison of hardness values measured by different methods), the results obtained were evaluated taking into account statistical analysis for the correctness of the data obtained. In order to further assess the homogeneity of the matrix structure, Vickers microhardness

Preprints (www.preprints.org) | NOT PEER-REVIEWED | Posted: 26 November 2020 doi:10.20944/preprints202011.0670.v1

tests were performed, in various areas of the blades, using the SHIMADZU-DORERNST M hardness tester with a load of 25G.

A static tensile test, considered a destructive test, was carried out with the Instron 8501 Plus universal testing machine in accordance with PN-EN ISO 6892-1:2010 standard. Due to the non-standardized, small dimensions of the strength specimens obtained (Figure 7.), in order to execute the static tensile test it was necessary to design and manufacture special holders enabling proper performance of the test (Figure 9.).

Figure 9. View of the test sample in specially designed holders.

The manufactured tooling made it possible to determine the following basic strength parameters based on the obtained tensile curves:

- 0.2 % offset yield strength $R_{0,2}$,;
- ultimate tensile strength R_m,
- fracture strain of sample A,
- Young's modulus E .

3. The results of tests

The microscopic observations carried out at magnifications of 100-10000x (Figure 10) showed that the TWC blade material is characterized by a multiphase structure typical for nickel-based heat-resistant alloys, after the supersaturation and aging process, consisting of the original grains of the solid solution γ (Figure 10. a) with cuboidal ultrafine grain precipitates of the γ 'intermetallic phase (Figure 10.b), as well as reinforcing carbides with the morphology of "Chinese script" (Figure 10.c).

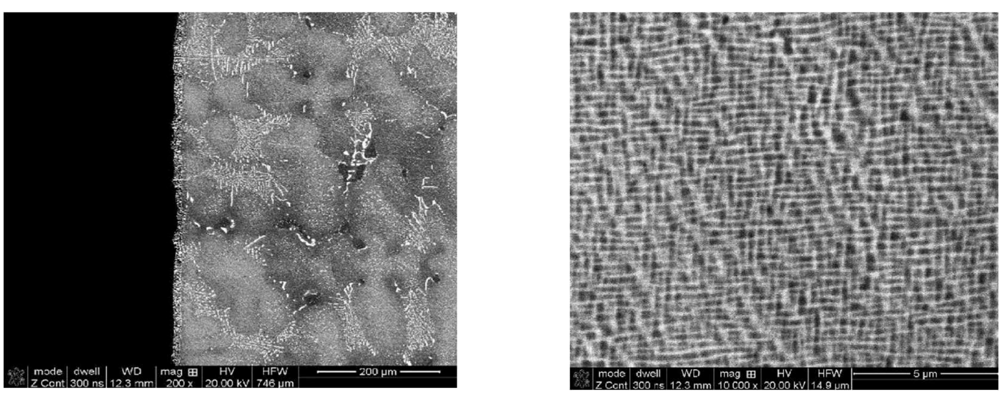

(a) (b)

 doi:10.20944/preprints202011.0670.v1

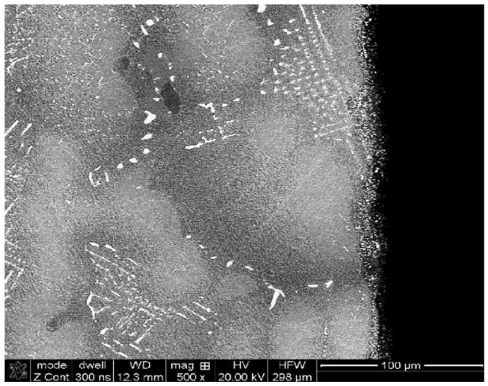

(c)

Figure 10. Multiphase structure of the TWC blade material built on the matrix of the γ phase (a) with cuboidal precipitates of the intermetallic phase γ ′ (b) and reinforcing carbide precipitates (c).

The available data shows that the blades of the turbine of the RD-33 engine are currently made of two types of alloys: monocrystalline ZhS-32 or directionally crystallized Zhs-26. Nevertheless, the microanalysis of the chemical composition of the multi-phase blade structure allowed to identify significant discrepancies, mainly in terms of the content of chromium and titanium, between the material tested and the alloys ZhS-32 and ZhS-26. The chemical composition of the analyzed material of the blades suggests that they are made of an alloy with a chemical composition corresponding to the heat-resistant nickel-based superalloy MAR-M 200 [9], which also corresponds to the chemical composition of the Russian ZhS-6U alloy [10] (Figure 11.).

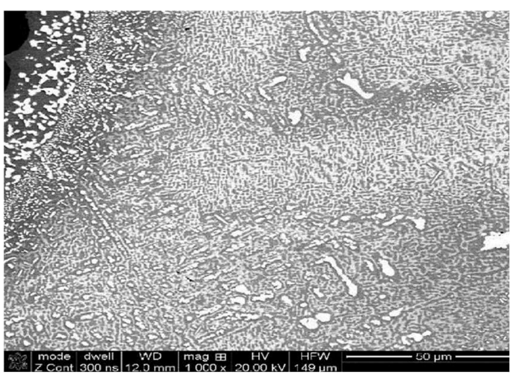

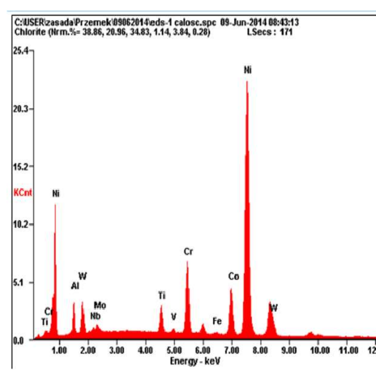

Element	Wt %	At %
AlK	06.67	14.36
NbL	01.32	00.83
MoL	01.84	01.12
TiK	02.75	03.34
V K	00.07	00.08
CrK	08.69	09.72
FeK	00.24	00.25
CoK	09.72	09.59
NiK	57.87	57.29
W L	10.81	03.42

(a) (b)

c) weight percentage (%) of individual alloy elements

	Ni	Cr	Co	Fe	Al	Ti	Mo	Nb	W	Ta	Re
material tested	57,87	8,69	9,72	0,24	6,67	2,75	1,84	1,32	10,81	---	---
MAR-M 200	59	9	10	<1	5	2	-	1	12,5	---	---
ZhS -6U	59,5	8,8	10,3	2	5,5	2,6	1,6	-	9,7	---	---
ZhS -32 Monocrystalline	residue	4,3-5,6	8,0-10,0	---	5,6-6,3	---	0,8-1,4	1,4-1,8	7,7-9,5	3,5-4,5	3,5-4,5
ZhS-26 directionally crystallized	residue	4,1-5,3	8,7-9,3	---	5,6-6,1	0,8-1,2	0,8-1,2	1,4-1,8	11,2-12	---	---

Figure 11. Result of microanalysis of the chemical composition of material of the HPT blade - the area subject to microanalysis (a) and the spectrum of identified elements (b) and commercial ember-resistant alloys of similar chemical composition (c).

Since the maximum exploitation temperature of the alloy MAR-M 200 is (according to the CES Edu Pack database) in the range 815-983°C and the temperature of the exhaust gases before the rotor wreath of a high pressure turbine (HPT) of the RD-33 engine reaches the upper level of the temperature range of the material used for the blades of HPT, therefore, in order to protect the material of the blade core it was covered with a barrier coating (Figure 12.) created by using the diffusional aluminizing technology.

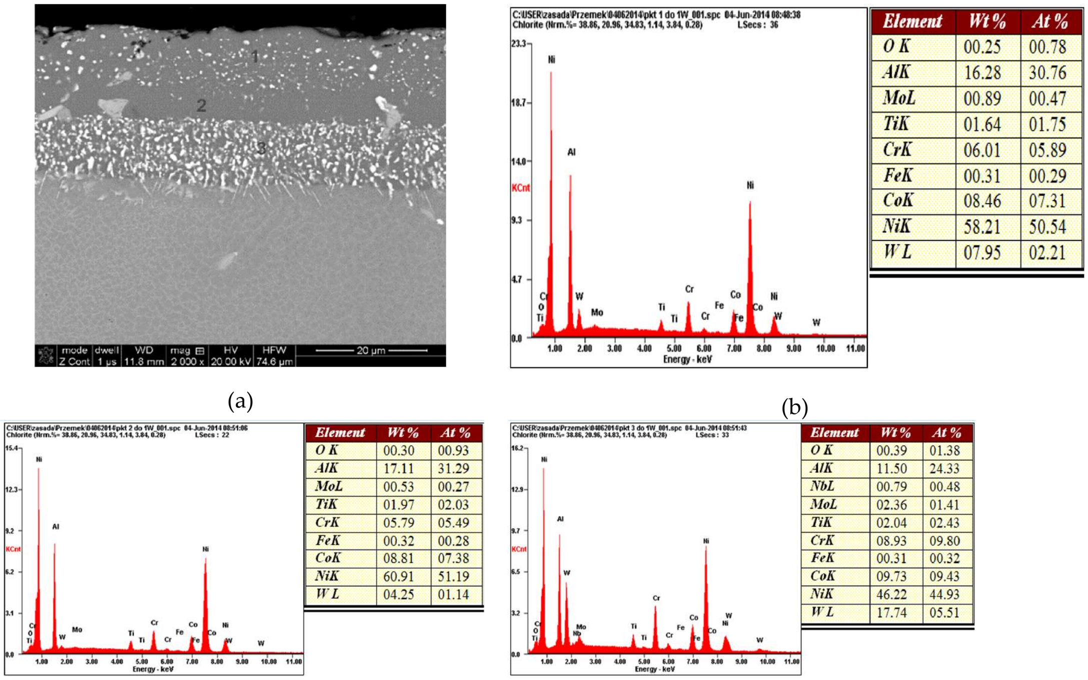

(b)

Element	Wt %	At %
O K	00.25	00.78
AlK	16.28	30.76
MoL	00.89	00.47
TiK	01.64	01.75
CrK	06.01	05.89
FeK	00.31	00.29
CoK	08.46	07.31
NiK	58.21	50.54
W L	07.95	02.21

(c)

Element	Wt %	At %
O K	00.30	00.93
AlK	17.11	31.29
MoL	00.53	00.27
TiK	01.97	02.03
CrK	05.79	05.49
FeK	00.32	00.28
CoK	08.81	07.38
NiK	60.91	51.19
W L	04.25	01.14

(d)

Element	Wt %	At %
O K	00.39	01.38
AlK	11.50	24.33
NbL	00.79	00.48
MoL	02.36	01.41
TiK	02.04	02.43
CrK	08.93	09.80
FeK	00.31	00.32
CoK	09.73	09.43
NiK	46.22	44.93
W L	17.74	05.51

Figure 12. Three-layer barrier nickel aluminides (NiAl) coating diffusively applied to the TWC blade material (a) and the results of microanalysis of the chemical composition in individual areas (b, c, d).

This process has led to the constitution on the surface of the blade material of a three-layer heat-resistant coating of NiAl intermetallic phase protecting the blade material from overheating.

Nevertheless, in spite of the material of the core of the HPT blade being protected against the temperature influence of exhaust gases, the barrier coating was damaged at the leading edge, which, due to temperature increase, led to changes in the grain structure of the blade at the overheating point. In addition to a small but noticeable growth of grains of the γ matrix from 80 up to 95μm, an anomalous selective growth and coagulation of precipitations of the γ' phase and an increase in the content of carbides in the structure are also observed, which may lead to a decrease of the creep resistance of the blade material.

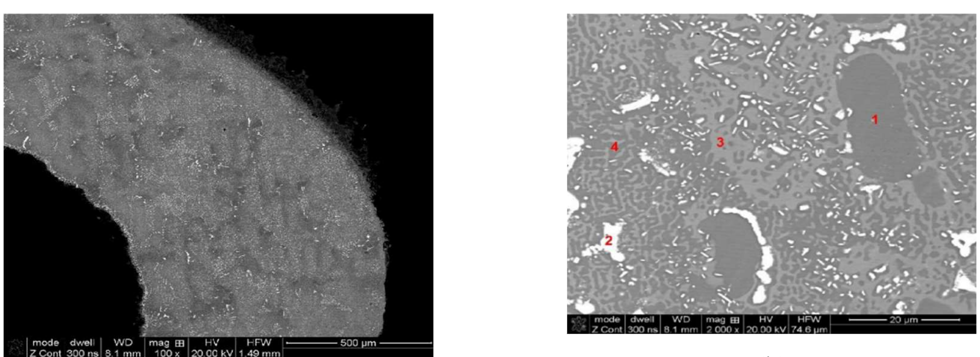

(a)

(b)

Preprints (www.preprints.org) | NOT PEER-REVIEWED | Posted: 26 November 2020 doi:10.20944/preprints202011.0670.v1

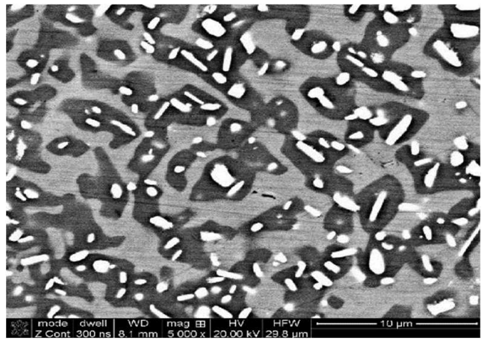

(c)

Figure 13. Damaged barrier coating at the leading edge of the HPT blade (a) and the effect of anomalous growth of the γ' phase (b) and increase in the share of carbides in the matrix of the core material (c) due to overheating.

Although the thermally less loaded material of the LPT blade coated with a diffusion barrier layer made of aluminides is also constructed of a multi-phased structure γ + γ' + MC, no abnormal growth of the superstructure γ' and carbides was observed in material of the LPT blade. A microanalysis of the chemical composition suggests that a similar phased composition to that of material of the HPT blade is the result of a similar chemical composition, suggesting that the same alloy was used for material of the LPT blade as in case of the HPT blade (Figure 14).

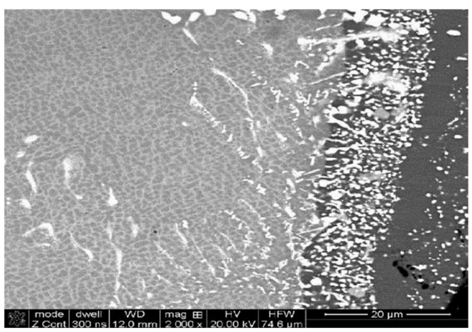

(a)

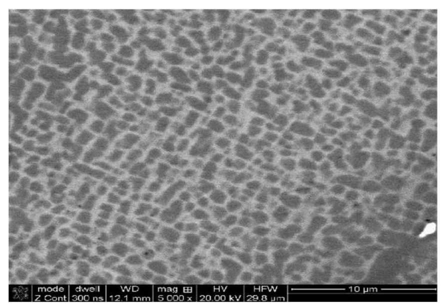

(b)

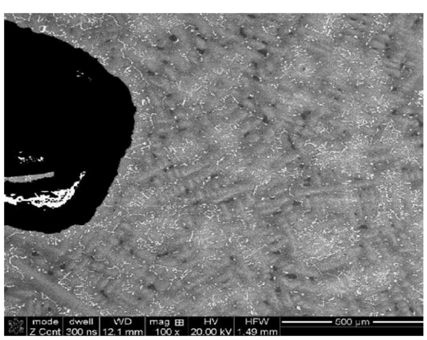

(c)

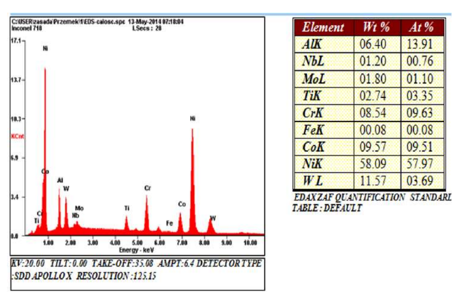

(d)

e)

	Weight percentage (%)								
	Ni	Cr	Co	Fe	Al	Ti	Mo	Nb	W
HPT blade	58,09	8,54	9,57	0,08	6,40	2,74	1,80	1,20	11,57
LPT blade	57,87	8,69	9,72	0,24	6,67	2,75	1,84	1,32	10,81

Figure 14. View of the structure of the LPT blade with barrier coating (a) with characteristic grain of the cuboidal phase γ' (b) and uniformly distributed reinforcing precipitations of carbides (c) and result of microanalysis of chemical composition the core material (d) and comparison with the microanalysis of material of the HPT blade (e).

The conducted microscopic observations made it possible to measure, by means of microscopic image analysis, the volume content of individual phases in the structures of the analyzed blades, as well as to assess the average grain size of the identified structural components. From the collected data presented in Table 2, it can be concluded that the structure of the material of the blades is stable as long as it is protected by a barrier coating.

Table 2. Volume content and grains size of individual phases in the structure of analyzed blades.

		HPT				HPT - overheated			LPT			
		LE int.	LE ext.	TE int.	TE ext.	LE int.	LE ext.	TE	LE int.	LE ext.	TE int.	TE ext.
γ	Content [%]	residue				residue			residue			
	Size [μm]	84,01		80,48		95,61		93,08	20,62	43,11	35,57	37,81
γ'	Content Share [%]	43,43	49,53	50,36	46,46	51,62	43,07	43,64	41,94		38,73	43,73
	Size [μm]	1,33	3,72	0,22	0,24	1,03	2,24	0,89	1,03	1,07	1,00	1,00
carbides	Content [%]	3,62	3,15	2,37	1,45	9,04	6,32	1,04	2,4		1,56	2,75
	Size [μm]	0,83	1,09	2,42	2,55	0,70	0,75	0,74	1,91	2,52	1,63	2,65

LE - leading edge; TE - trailing edge; int. - internal area (cooled); ext. - external area flushed by the exhaust gas stream

The damage to the protective layer, as already indicated, leads to a noticeable growth of the matrix grains and tripling increase of the carbide volume content.

Microscopic observations have been confirmed by the XRD analysis. Based on the X-ray phase analysis measurements, by analyzing the positions of the obtained reflections, it was possible to unequivocally confirm the multi-phase structure of the blade material observed during microscopic observations (Figure 15).

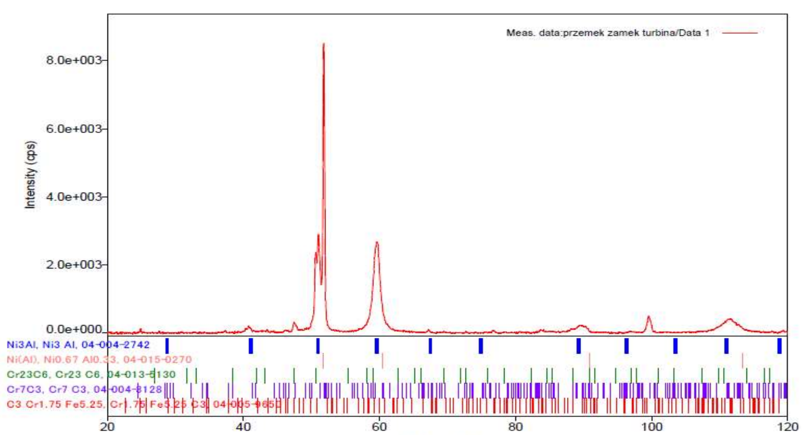

Figure 15. XRD pattern of blade material with identified phases.

The distribution of alloying elements suggested the occurrence of the three-phased structure of the material based on the solid solution of aluminum in nickel γ and of the areas of intermetallic phase γ' on the matrix of the Ni3Al superstructure and carbide precipitates, mainly Cr23C6, which

 doi:10.20944/preprints202011.0670.v1

was fully confirmed by the comparison analysis of obtained reflections[results?] with the data contained in PDF-4 database.

Additional evidence confirming the comparable structural-phase composition of the analyzed blades are microhardness measurements [7] carried out with the materials of the tested blades. These tests were carried out with the semi-automatic microhardness tester SHIMADZU-DORERNST M and the obtained results were subjected to statistical analysis which confirmed the structural homogeneity of the analyzed material areas, characterized by an average value of microhardness at a statistically uniform level within the range 410-430HV0.025 (Figure 16.).

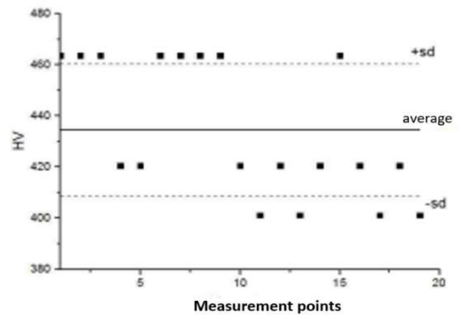

(a)

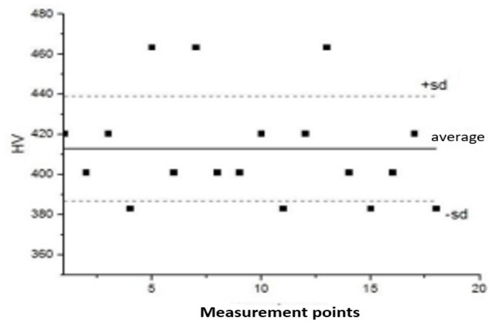

(b)

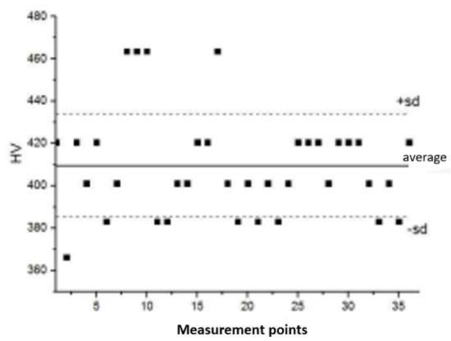

(c)

Figure 16. Statistical distribution of microhardnesses in material of the HPT blade in the overheated zone (a) in the non-overheated zone (b) and in material of the LPT blade.

The observed structural changes were reflected in the strength parameters of the alloy used for the construction of the tested blades. As can be seen in Figure 17, where the hardness values obtained were marked with the standard deviation determined, the intersection points (marked with green color) of the hardnesses obtained are located on the curves representing the dependency between Brinell and Rockwell hardness as the function of Vickers hardness (curves HB=f(HV) and HRB=f(HV)), which clearly proves the correctness of the measurements carried out. It also proves despite the multiphase nature of the tested material, its high homogeneity caused by the refinement of the grain structure.

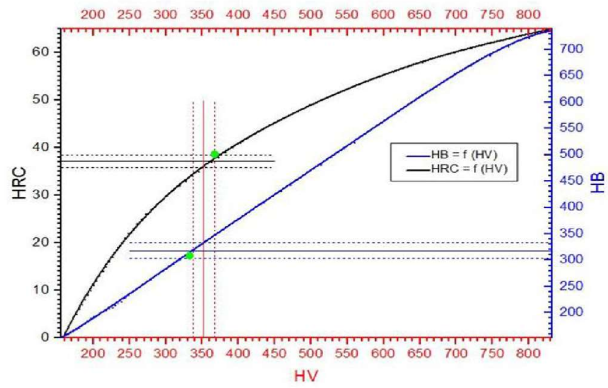

Figure 17. Comparison of hardness measurements obtained with the Rockwell PW 106 hardness tester and the Wolpert Wilson Testor 751 universal hardness tester.

However, the average value of hardness of the analyzed material after its exploitation has decreased to the level of 350HV10 compared to 450HV10, which is characteristic in case of the correct structure of the ZhS-6U alloy.

It should also be noted that the values of hardness (Figure 17.) and microhardness (Figure 16.) measured by the same Vickers method differ significantly, reaching 70 HV hardness units in extreme cases. However, the observed phenomenon, indentation size effect (ISE), is in accordance with the variable hardness law, which describes the influence of elastic deformation on the value of obtained results, i.e. the smaller the load, the greater the influence of elastic deformation and thus the greater the value of hardness. At this point it should be recalled that the load for microhardness measurements was 25G and for hardness measurements was 10kG.

The decrease in strength properties is confirmed by the results of the static tensile test (Figure 18).

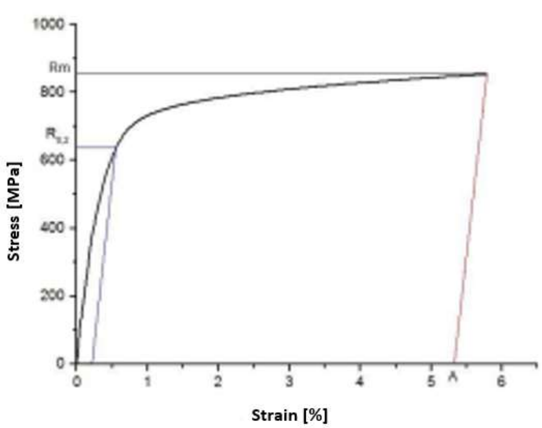

(a)

(b)

	1	2	3	Average	SD	
$R_{0,2}$	643	743	650	**678**	**55**	[MPa]
R_m	851	870	899	**873**	**24**	[MPa]
E	213	219	220	**217**	**3,8**	[GPa]
A	5,3	5	10,38	**6,9**	**3,0**	[%]

Figure 18. Tensile curve of blade material (a), view of specimens before and after the tensile test (b) and determined strength parameters.

The decrease in the share of the γ 'phase in the material structure and there is growth, caused, in accordance with the Hall-Petch relationship, a decrease in the yield point from the original level of 770MPa for the ZhS-6U alloy to 678MPa of the material of the tested blade (Table 3).

Table 3. Strength properties at room temperature of nickel-based superalloys potentially used to construct HPT blades and LPT blades of the engine RD33.

	E [GPa]	HV	R_{02} [MPa]	R_m [MPa]	A
Żs-32	244	466	850	880	13,0
Żs-26	253	480	790	1000	6,8
Żs-6U	240	450	770	830	3,0
MAR-M200	230	---	860	960	7,0
Material tested	217	350	678	873	6,9

4. Summary

The data obtained as a result of material tests of blades of rotors of the low and high pressure turbine of the RD-33 engine, taking into account the chemical composition and the phase structure corresponds to the Russian alloy, the type Zhs-6U, used in the early versions of the RD-33 engine. The deployment of blades made of the ZhS-26 and ZhS-32 alloys allowed to increase the temperature of exhaust gases before the turbine, thus increasing the engine performance. However, the conscious or unconscious use, in this exploitation conditions, of blades made of ZhS-6U alloy with noticeably lower structural stability, combined with local damage to the barrier protective coating, resulted in a distinctive, more than 10 per cent reduction of strength properties, primarily plasticity limit, which could ultimately lead to engine failure and even damage to the engine.

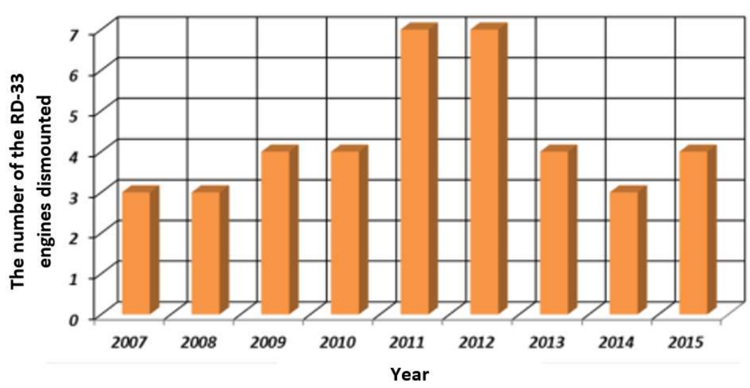

Figure 19. The number of the RD-33 engines dismounted from the airplanes due to damages to the high pressure turbine in one of the air bases in Poland in the years 2007-2015 [11.].

The values of the determined strength parameters will be used in further work related to numerical analyses in the field of strength issues concerning the life and failure of engines manufactured by Russia, including the RD-33 engine. The importance and need for such works [3.], [11.], [12.] may be proved by the number of RD-33 engines dismounted from the airplanes in one of the air bases due to the damages in the high pressure turbine, which is shown in the diagram in Fig. 19. In addition, the analysis of structural changes caused by exploitation conditions can be helpful in the search for and selection of material substitutes, used to construct the engine element under analysis, which will meet increasingly higher, mainly temperature-related design requirements.

References

1. Игоревич Х. И., Разработка экономнолегированного никелевого жаропрочного сплава для монокристаллического литьярабочих лопаток ГТД, Рыбинск – 2017

 doi:10.20944/preprints202011.0670.v1

2. Каблов Е.Н., Орехов Н.Г., Толораия В.Н., Демонис И.М., Литейные жаропрочные сплавы н технология получения монокристаллических турбинных лопаток ГТД , ВИАМ Москва 2001
3. Čerňan J., Janovec M., Hocko M., Cúttová M., Damages of RD-33 Engine Gas Turbine and their Causes, *Transportation Research Procedia* Volume 35, 2018, p.p 200–208
4. Каблов Е.Н., Петрушин Н.В., Компьютерный метод конструирования литейных жаропрочных никелевых сплавов, *Авиационные Материалы и Технологии* 1/2004, ISSN:2071-9140
5. Скубачевский Г. С., Авиационные газотурбинные двигатели, Moskwa, *Машиностоене* 1981
6. Сиротин Н. Н., Контроль u дигатностика технического состояния газотурбинных двигательей, *Машиностроение*, Москва 2007.
7. Kurzydłowski K.J., "Rozwój materiałów konstrukcyjnych: Historia stopów aluminium" Sesja z okazji 75-lecia Przeglądu Mechanicznego, 12 luty 2010, Warszawa;
8. Jakubowski R. "Teoria silników lotniczych - Rozwój i przegląd konstrukcji",
9. http://jakubowskirobert.sd.prz.edu.pl/file/MjMsNjcsMjcxLHRlb3JpYV9zaWxuaWtvd19sb3RuaWN6eWNoX3dwcm93YWR6ZW5pZS5wZGY=
10. Hernas A., Maciejny A., "Żarowytrzymałe stopy metali", Wydawnictwo PAN, Katowice 1989.
11. Kaibyshev O. A., "Superplasticity of Alloys, Intermetallides and Ceramics", Springer-Verlag Berlin Heidelberg 1992, ISBN-13 :978-3-642-84675-5
12. Trelka, M., Bartoszewicz, J., Urbaniak, R., Selected problems of RD-33 engine reliability in operation, Combustion Engines, 2016, 165(2), 33-40
13. SILADIC M., RASUO B., On-Condition Maintenance for Non-Modular Jet ENGINES - an Experience, ICAS 2008, 26TH International Congress of THE Aeronautical Sciences